OPO OPHTHALMIC AND PHYSIOLOGICAL OPTICS
THE JOURNAL OF THE COLLEGE OF OPTOMETRISTS

Ophthal. Physiol. Opt. 2009 **29:** 281–287

The contribution of the fixational eye movements to the variability of the measured ocular aberration

J. Arines[1], E. Pailos[2], P. Prado[2] and S. Bará[2]

[1]Departamento de Fisica Aplicada (área de óptica), Facultad de Ciencias, Universidad de Zaragoza, c\ Pedro Cerbuna 12, 50009 Zaragoza, and [2]Departamento de Fisica Aplicada (área de óptica), Universidade de Santiago de Compostela, Escola Universitaria de Óptica e Optometría, Santiago de Compostela (Galicia), Spain

Abstract

The purpose of this work is to analyze the contribution of eye movements to the variability of the Zernike coefficients as determined with a Hartmann–Shack aberrometer. In order to isolate this effect we considered static aberrations tied to the eye pupil. We used several eye movements of different magnitude, both synthetic and corresponding to actual series recorded in our laboratory with different subjects. Our results show the relevance of the modal coupling induced by the estimation process and the benefit of correcting eye movements in order to get a better estimate of the ocular aberrations. They also show that eye movements during aberrometric measurements are an important source of apparent wavefront variability.

Keywords: fixational eye movements, Hartmann-Shack, ocular aberrometry, wavefront estimation

Introduction

Eye movements, both voluntary and involuntary, are a key factor in human vision. During steady-state fixation, the eye shows involuntary eye movements that exhibit an erratic trajectory with three main components: drifts, a slow component with amplitude of 0.02°–0.15°; fast microsaccades, with 25 ms duration, amplitude of 0.22°–1.11° and frequency of 0.1–0.5 Hz; and tremors, with very low amplitude (0.001°–0.008°) but very high frequency (50–100 Hz) (Abadi and Gowen, 2004; Møller *et al*., 2006).

Fixation characteristics and thus eye movement properties depend on patient attention. Several studies have shown that saccadic movements are affected by endogenous and exogenous sources, and that the magnitude of this influence on fixational eye movements is highly subject-dependent (Gowen *et al*., 2007).

Received: 3 November 2008
Revised form: 19 January 2009
Accepted: 2 February 2009

Correspondence and reprint requests to: J. Arines.
Tel.: +34 976762849; Fax: +34 976761233.
E-mail address: fajap@unizar.es

During recent years much effort has been devoted to attempts to understand the sources of variability of the ocular aberrations. Tear film dynamics, retinal pulsation, and microfluctuations of accommodation are some of the sources that have been identified (Kotulak and Schor, 1986; Hofer *et al*., 2001; Montes-Mico *et al*., 2004; Zhu *et al*., 2004).

However, the understanding of ocular aberration dynamics is still incomplete. In our opinion there is a further source of variability that should be taken into account: the ocular movements that occur while looking at the fixation target during the measurement of the ocular aberrations. We consider this source as an extrinsic one. The reason is that these small-magnitude rotational ocular movements induce an effective translation of the eye pupil over its plane, and although they do not affect the ocular aberration they cause a change in the estimated wavefront coefficients.

The vector of coefficients that describe any ocular wavefront is the result of projecting the latter over a set of Zernike polynomials defined with respect to a certain reference system. Any change in the position of the ocular wavefront with respect to the reference frame will cause the set of coefficients to be modified.

doi: 10.1111/j.1475-1313.2009.00663.x

When measuring ocular aberrations we can define two reference frames: the wavefront sensor reference frame (WSRF), which is tied and centred with respect to the aberrometer sampling element (the microlens array of Hartmann–Shack aberrometers or the pupil sampling diagram of Laser Ray Tracers); and the eye reference frame (ERF), which is tied and centred with the eye pupil (see *Figure 1*). In most current wavefront sensors the estimation is performed with respect to the WSRF. Bear in mind that pupil decentring might occur during measurement acquisition, even though the eye was centred at the beginning of the sequence. As a consequence of this, estimation of the wavefront with respect to the WSRF has an important drawback: any pupil movement causes a significant variation of the estimated coefficients obtained in this measurement frame.

In contrast with the situation described above, if the position of the eye pupil relative to the reference frame used for the estimation is kept constant (as occurs when using the ERF), the variability of the estimated coefficients would be reduced to that caused by the different modal coupling induced by changing the coordinates of the sampling elements with respect to the incident wavefront and also the ERF (Hermann, 1981).

This paper will show the importance of estimating the ocular aberration with respect to the ERF in order to reduce the variability of the estimated wavefront coefficients. Better estimates of the statistical properties of ocular aberration and improvements in the design of customized refractive compensation of ocular aberrations can easily be achieved. What will also be clear is that eye-trackers should be included in wavefront-sensing arrangements, in order to provide correct estimates of the relative position of the eye pupil with respect to the WSRF (and the sampling array) and, as a result, to allow wavefront estimation with respect to the ERF.

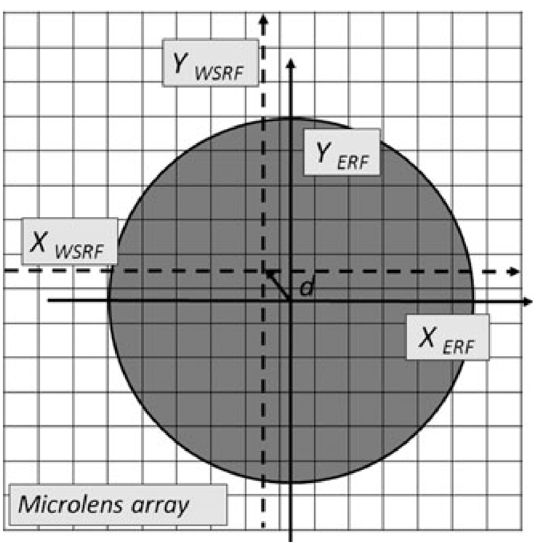

Figure 1. Wavefront sensor reference frame (WSRF), and eye pupil reference frame (ERF).

In the first section of this work we present a description of the computer simulation. Then, in the result sections we analyze first the contribution of fixational eye movements to the variability and bias of the estimated Zernike coefficients. Second, we show the relation between the root-mean-square (rms) error of the estimated wavefront and the centre of the ocular trajectory. Additionally, we show the influence of the modal coupling induced in the estimation process on the reconstruction error. Finally, we present a discussion of the results.

Description of the computer simulation

We simulated two hypothetical eyes with static aberrations. The wavefront aberration was generated with Zernike polynomials up to the 12th order (91 polynomials). In order to compute the value of the Zernike coefficients we used the following procedure. First, we measured with a Hartmann–Shack aberrometer the first 35 polynomials of the ocular aberration of two subjects. Then, we calculated the variance of each radial order, from the 2nd to the 7th, using the following expression, $\hat{\sigma}_n^2 = \sum_{all\ m} \hat{a}_{n,m}^2$, where the hat stands for estimated or experimental magnitudes. Next, an exponential function $\sigma_n^2 = b\exp(-cn)$ was fitted to the values of the experimental variance. The decays (c) obtained for both eyes are compatible with those recorded by Thibos *et al.* (2002), who established an exponential decrease of the coefficients' variance with the radial order. The knowledge of the variance trend allows us to obtain variance values to orders beyond those experimentally available, for example up to the 12th order, which are of interest when assessing the impact of modal coupling. Coefficients of the static aberration with respect to the ERF were then randomly generated for a 5 mm pupil diameter, using a Gaussian statistical model with zero mean and an order-depending variance given by the experimental fit: $\sqrt{\sigma_n^2/(n+1)}$, where n is the radial order. The root-mean-square value of the generated coefficients from 36th to 91st polynomial, called in this paper 'very high order rms' (rms_{VHO}), of the synthetic eye A is four times bigger than that of eye B (see *Table 1*).

Table 1. Simulation parameters

Microlens array	89 in square lattice
Microlens side	450 μm
Pupil diameter	5 mm
Eye A rms_{VHO}	0.0176 μm
Eye B rms_{VHO}	0.0046 μm

A Hartmann–Shack wavefront sensor was also simulated. Table 1 shows its characteristics. Measurement error was not considered in the simulation. Exact knowledge of the pupil translation was assumed when performing the estimation in the ERF. Fifty sets of pupil trajectories were used in the simulation, each of them with 50 positions. Two of the trajectories were obtained experimentally in our laboratory.

The synthetic ocular trajectories were computed using the random-walk model (Engbert and Kliegl, 2004). Inside each trajectory every position was generated by adding a random value to the previous position (see *Equation 1*):

$$\vec{x}_k = \vec{x}_{k-1} + \Delta\vec{x}_k, \quad (1)$$

where $\vec{x}_k$ and $\vec{x}_{k-1}$ are the coordinates of the pupil centre at the *kth* and *kth*-1 positions, and $\Delta\vec{x}_k$ is a random Gaussian variable of zero mean and a specified standard deviation (in this work we assumed a value of 20 μm). Refixation of the target was included in the simulation when decentrations with respect to the first position of the sequence were bigger than 200 μm. The initial position and the refixated ones were randomly generated following a Gaussian distribution of zero mean and a standard deviation of 20 μm. In *Figure 2* we show the 50 trajectories, some of them being emphasized.

Estimation of the modal coefficients was carried out using the least-squares approach (Hermann, 1981). We used the same vector of measurements to estimate two vectors of coefficients of different length, 36 and 66 elements respectively, in order to study the effect of modal coupling (Hermann, 1981).

In order to obtain the modal coefficients of the wavefront expansion for each of the positions we employed a translation matrix of dimensions consistent with the size of the coefficient vector (91 × 91) computed as described in Bará *et al*., 2006. The same procedure was used to compute the translation matrix used to obtain the modal coefficients in the ERF from those estimated in the WSRF. In this case the dimensions were 35 × 35 or 66 × 66 depending on the size of the estimated coefficient vector.

In the next section we include the different results that we obtained from the numerical simulation. We show first the influence of the ocular movements on the mean and variance of the measured coefficients. Then, we focus on presenting the correlation found between the trajectory's centre and the root-mean-square difference between the original wavefront and the estimated one (*rms* error). Finally, we assess the benefit of expressing the estimated wavefront with respect to a reference frame tied to the eye pupil (ERF) and its dependence on the modal coupling induced in the estimation process.

Results

Mean values and standard deviations of the coefficients

In this section we study the influence of the ocular movement on the mean value and variance of the estimated coefficients of the wavefront's Zernike expansion. We considered the hypothetical eye B with a static wavefront aberration and an erratic movement (as we mentioned in the description of the simulation). We estimated 66 Zernike coefficients of the wavefront aberration expansion for the 50 different positions along the two real eye trajectories measured in our laboratory and represented in *Figure 3*. Then, we computed the mean value and the variance of each of the estimated Zernike coefficients.

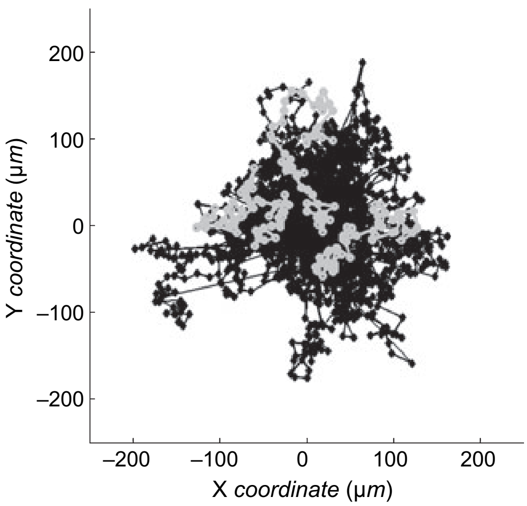

Figure 2. Fifty simulated trajectories of translational movements of the entrance pupil centre of the eye.

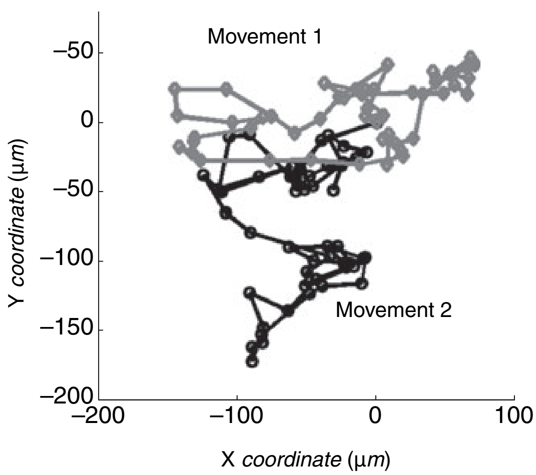

Figure 3. Experimental pupil centre movements 1 and 2, as registered during aberrometric measurements.

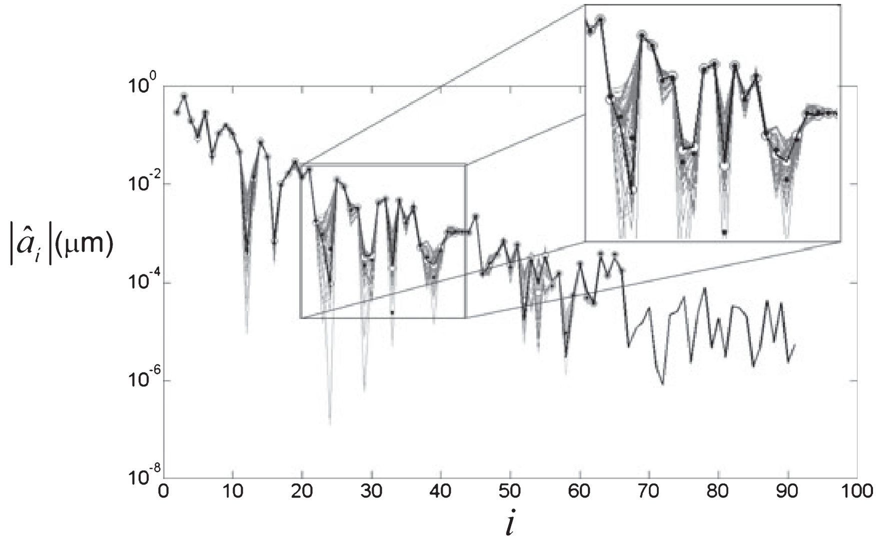

Figure 4. Absolute values of the estimated coefficients for movement 1. i is the Zernike modal order. The graph shows the values obtained for each of the 50 positions along the pupil trajectory as well as the mean values of the coefficients. The dark grey lines show the results for the WSRF, the light grey lines for the ERF. Black dots represent WSRF mean values, white dots ERF mean values. The black line shows the original static coefficients.

Figure 4 shows the results obtained for the movement 1. We show in this figure the absolute value of the estimated coefficients with respect to the wavefront sensor's and eye's reference frame (WSRF, ERF) as a dark grey line and light grey line, respectively. Black dots represent the WSRF mean values, and white dots the ERF mean values; the black line shows the original static coefficients. A magnified section of the graph is superimposed in order to show the bias in the estimation of the mean value in the WSRF and ERF.

We can see in *Figure 4* that eye movements cause the estimated Zernike coefficients to differ significantly from their static values, the differences in absolute value being significantly higher for the coefficients estimated with respect to the WSRF. The coefficients of the 9th order are the same in both reference frames due to the superior triangular form of the translation matrix (see Arines *et al.*, 2008).

In *Figure 5* we show the standard deviations of the estimated coefficients with respect to the wavefront sensor (in black) and the eye (in grey) reference frames, for movement 1. The standard deviation decreases with increasing Zernike mode index for the coefficients estimated in the WSRF, while for those computed with respect to the ERF the standard deviation shows little change.

From *Figures 4 and 5* we can conclude that the movement of the eye induces uncertainty and variability to the estimated coefficients. This uncertainty and variability can be reduced by estimating the modal coefficients with respect to the eye's reference frame (ERF).

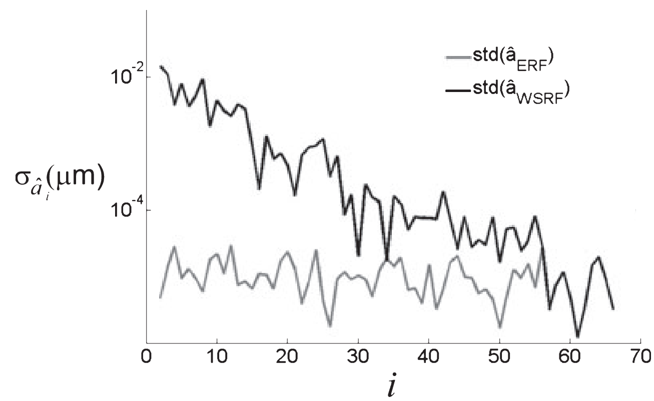

Figure 5. Standard deviation of the coefficients estimated in the WSRF (black) and ERF (gray) for eye B.

Pupil decentration and residual rms

In order to analyze the relation between the eye movement and the uncertainty in the coefficient estimation we show in *Figure 6* the *rms* error ($rms|_{W-\hat{W}}$) vs the mean radial decentration of each trajectory (r_j), defining both magnitudes by the following expressions:

$$rms|_{W-\hat{W}} = \sqrt{\left\langle \sum_{i=0}^{M} (a_i - \hat{a}_i)^2 \right\rangle}, \tag{2}$$

$$r_j = \left\langle \sqrt{x_j^2 + y_j^2} \right\rangle, \tag{3}$$

where $a_i, \hat{a}_i$ are the modal coefficients of the wavefront and the estimated ones for every pupil position; x_j, y_j

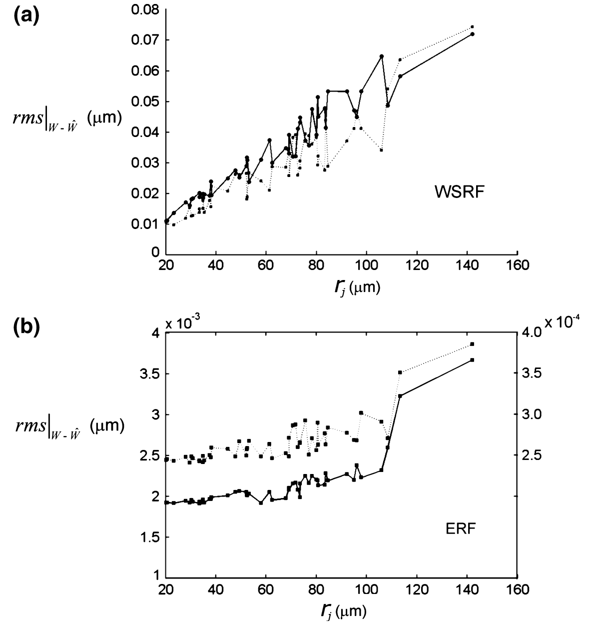

Figure 6. Residual root-mean-square error, $rms|_{W-\hat{W}}$, vs mean trajectory decentration, r_j, for the coefficients obtained in the WSRF (a) and ERF (b). The solid black line refers to the case of eye A and the dotted black line to eye B.

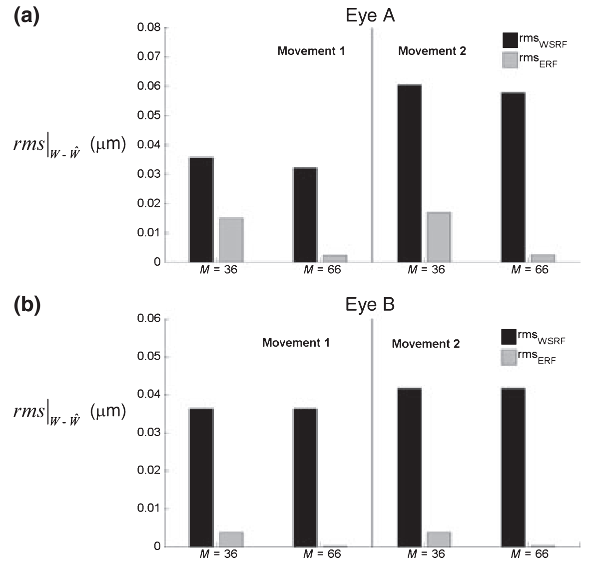

Figure 7. Root-mean-square differences between the original and estimated wavefront in the WSRF and ERF for eyes A (a) and B (b), and movements 1 and 2.

are the coordinates of the positions of the *j-th* trajectory; and $\langle\rangle$ is the mean value over the positions of each trajectory. The $rms|_{W-\hat{W}}$ was evaluated for 50 synthetic trajectories (with 50 positions along each trajectory). In *Figure 6a, b* we represent the $rms|_{W-\hat{W}}$ computed for the coefficients estimated in the WSRF and the ERF, respectively. We also compare the results obtained for the eyes A (solid black line) and B (dotted black line); the grey scale of the right hand side of *Figure 6b* corresponds to the results for eye B. It will be remembered that these eyes present a significant difference in the magnitude of their very high-order coefficients (see *Table 1*). We can see in *Figure 6* the clear correlation between the $rms|_{W-\hat{W}}$ and the mean radial decentration, r_j. We can also see that this dependence can be greatly reduced by estimating the coefficients with respect to the ERF, achieving a nearly constant $rms|_{W-\hat{W}}$ up to 80–90 μm of radial decentration. In addition, *Figure 6b* shows a difference between the values of the $rms|_{W-\hat{W}}$ computed for eye A and eye B of nearly one order of magnitude. This result emphasises the importance of the amount of the high-order aberration for the individual eye when evaluating the influence of the ocular movement on the $rms|_{W-\hat{W}}$.

ERF & WSRF estimation

In this section we show a comparison of the estimation process performed in both the sensor (WSRF), and eye (ERF) reference frames. Two different hypothetical eyes with different aberration (Eyes A and B, see *Table 1*) were supposed to follow two different trajectories (see *Figure 3*). We also estimated two different sets of coefficients in each case, one with 36 coefficients and other with 66, with the aim of analyzing the contribution of modal coupling (i.e. the redistribution of the contribution of the non-estimated Zernike coefficients among the estimated coefficients (Hermann, 1981)).

The parameter used for the comparison was the *rms* error ($rms|_{W-\hat{W}}$), see *Equation 2*. The ERF coefficients were obtained by multiplying the coefficients estimated in the WSRF by a translation matrix computed using the algorithm proposed by Bará *et al*. (2006).

In *Figure 7* we show the results. In black we present the values of $rms|_{W-\hat{W}}$computed with the coefficients estimated in the WSRF and in gray the ones obtained with those computed in the ERF. *Figures 7a, b* correspond to eyes A and B, respectively.

If we compare the graphs of *Figure 7a* we can observe that $rms|_{W-\hat{W}}$ depends highly on the ocular movement, being significantly smaller for movement 1 (compare each bar in the left box of *Figure 7a* with the same color, corresponding bar in the right box). If we compare movement trajectories 1 and 2 (*Figure 3*), we observe that the second one is more decentred and wider. However, if we pay attention to *Figure 7b* (eye B), we see that the difference between the $rms|_{W-\hat{W}}$ obtained for both movements is less significant. This means that the influence of the eye movement on the estimated coefficients depends not only on the characteristics of the movements but also on the magnitude of the high-order aberration (HO) of the particular eye. Remember that the rms_{VHO} of eye B is four times lower than that of eye A.

From *Figure 7* we can also notice a difference in the magnitude of the $rms|_{W-\hat{W}}$ obtained in the WSRF and in the ERF for each eye and trajectory (compare every black bar with its adjacent gray one). Besides, there is a significant difference in the magnitude of the $rms|_{W-\hat{W}}$ between both eyes under similar conditions (compare each bar in *Figure 7a* with the corresponding bar in *Figure 7b*). In the case of eye B the $rms|_{W-\hat{W}}$ in the ERF is nearly negligible (see the gray bars in *Figure 7b*). Additionally, if we compare the $rms|_{W-\hat{W}}$ obtained when estimating 36 and 66 coefficients in the ERF for each eye and movement, we again find an important difference (compare the gray bars inside each box of either figure).

Discussion

Throughout this paper we have analyzed the influence of ocular movements on the estimated Zernike coefficients. To do that, we simulated two hypothetical eyes, with different static aberrations and a significant difference in the magnitude of their high-order aberrations, following several trajectories.

All the results presented in this paper underline the influence of the ocular fixational movements on the estimated coefficients, and thus on the statistical properties atributed to the dynamics of ocular aberrations and the population distribution of Zernike coefficients.

Figure 4 shows the different values of the Zernike coefficients obtained when measuring the static wavefront following an erratic trajectory typical of that of fixational eye movements. The non-zero mean distribution of positions causes a bias in the estimation of the static aberration. The better accuracy and precision (see *Figure 5*) achieved when the coefficients are estimated with respect to the eye's reference frame, ERF (thanks to the correction of the movement by multiplying the WSRF coefficients vector by a translation matrix, see Bará *et al*., 2006 and Arines *et al*., 2008), suggest the importance of correcting the estimated coefficients in order to get a better understanding of the statistical properties of the dynamics of the ocular aberrations.

As we said in the previous paragraph, the non-zero mean of the trajectory positions causes bias in the value of the estimated coefficients. *Figure 6* shows that relation. In contrast to the high correlation that can be observed between the trajectory centre and the mean value of the coefficients estimated in the WSRF (see *Figure 6a*), we observe in *Figure 6b* that, up to 80–90 μm of decentration, the *rms* in the ERF is almost constant. Another difference between *Figure 6a, b* that should be pointed out is the magnitude of the *rms*, one order of magnitude. This difference is significant, and is important when we are trying to understand the sources of variability of the ocular aberrations or to know their statistical properties.

One question that remains open after reading the previous paragraph is: why can we only correct properly the displacements smaller than 80–90 μm? (see *Figure 6b*). Initially, we would expect to be able to obtain a good correction, independent of the magnitude of the displacement. The answer to this question deals with the modal coupling mentioned in previous sections. The translation matrix applied to the coefficients estimated with respect to the WSRF can correct the variability induced by the ocular displacements, but it does not prevent the changes in the amount of modal coupling. *Figure 7* supports this explanation. The *rms* error depends on the magnitude of the very high order aberration (the rms_{VHO} of eye A is four times higher than that of eye B), on the movement, on the number of modes estimated and thus on the modal coupling, and on the system of reference used to estimate the coefficients. The higher the number of modes estimated, the lower the modal coupling and, as can be seen in *Figure 7*, the correction of the movements is better.

In conclusion, the results presented in this paper show the contribution of fixational ocular movements to the variability and loss of precision and accuracy of the estimated modal coefficients. Consideration of these movements and their correction by expressing the wavefront coefficients with respect to a reference frame tied to the eye pupil is necessary for a better understanding of the ocular aberration and statistical properties. We think that the use of eye trackers should be considered in order to measure the eye position during aberrometric measurement to compensate – at least partially – for this source of error.

Acknowledgements

Spanish Ministerio de Educación y Ciencia, grant FIS2005-05020-C03-02, the European Regional Development Fund. Eliseo Pailos holds a FPU scholarship awarded by Ministerio de Ciencia e Innovación.

References

Abadi, R. V. and Gowen, E. (2004) Characteristics of saccadic intrusions. *Vision Res.* **44,** 2675–2690.

Arines, J., Prado, P., Bará, S. and Acosta, E. (2008) Equivalence of least-squares estimation of eye aberrations in linearly transformed reference frames. *Opt. Commun.* **281,** 2716–2721.

Bará, S., Arines, J., Ares, J. and Prado, P. (2006) Direct transformation of Zernike eye aberration coefficients between scaled, rotated, and/or displaced pupils. *J. Opt. Soc. Am. A* **23,** 2061–2066.

Engbert, R. and Kliegl, R. (2004) Microsaccades keep the eye's balanced during fixation. *Psychol. Sci.* **15,** 431–436.

Gowen, E., Abadi, R. V., Poliakoff, E., Hansen, P. C. and Miall, R. C. (2007) Modulation of saccadic intrusion by exogenous and endogenous attention. *Brain Res.* **1141,** 154–167.

Hermann, J. (1981) Cross coupling and aliasing in modal wave-front estimation. *J. Opt. Soc. Am.* **71,** 989–992.

Hofer, H., Artal, P., Singer, B., Aragón, A. L. and Williams, D. R. (2001) Dynamics of the eye's wave aberration. *J. Opt. Soc. Am. A* **18,** 497–506.

Kotulak, J. C. and Schor, C. M. (1986) Temporal variations in accommodation during steady-state conditions. *J. Opt. Soc. Am. A* **3,** 223–227.

Møller, F., Laursen, M. L. and Sjølie, A. K. (2006) The contribution of microsaccades and drifts in the maintenance of binocular steady fixation. *Graefe*'s Arch. Clin. Exp. Ophthalmol. **244,** 465–471.

Montes-Mico, R., Alio, J. L., Muñoz, G. and Charman, W. N. (2004) Temporal changes in optical quality of air-tear film interface at anterior cornea after blink. *Invest. Ophthalmol. Vis. Sci.* **45,** 1752–1757.

Thibos, L. N., Hong, X., Bradley, A. and Cheng, X. (2002) Statistical variation of aberration structure and image quality in a normal population of healthy eyes. *J. Opt. Soc. Am. A* **19,** 2329–2348.

Zhu, M., Collins, M. J. and Iskander, R. (2004) Microfluctuations of the wavefront aberrations of the eye. *Ophthalmic Physiol. Opt.* **24,** 562–571.